Pergamon

Int. J. Heat Mass Transfer. Vol. 40, No. 17, pp. 4161–4168, 1997

0017–9310/97 $17.00+0.00

PII: S0017-9310(97)00020-3

Thermal streaks regeneration in the wake of a disturbance in a turbulent boundary layer

G. HETSRONI, A. MOSYAK and L. P. YARIN

Department of Mechanical Engineering, Technion—Israel Institute of Technology, Haifa, Israel

(*Received* 11 *March* 1996 *and in final form* 9 *January* 1997)

Abstract—The temperature field on the surface of a wall, in the wake of a rib placed in the spanwise direction, is studied by using infrared thermography. Experimental data on distribution of the heat transfer coefficient are present for various Reynolds numbers, as well as for different inclinations of the rib to the wall. The effect of flow perturbations on the temperature of the surface is studied. A phenomenological model is proposed to describe the evolution of the temperature field. © 1997 Published by Elsevier Science Ltd.

1. INTRODUCTION

The work reported here is aimed at enhancing the heat transfer in a turbulent boundary layer. Among the various methods of heat transfer improvement, there is the method based on the perturbation of the near-wall flow by means of a rib oriented in the spanwise direction [1–3].

The effect of ribs on convective heat transfer in turbulent boundary layer was the subject of numerous investigations in the past decade [4–14].

These studies contain data on the hydrodynamic and thermal structure of flow near a single rib or array of ribs, such as velocity and temperature distributions over the ribbed surface, heat transfer coefficient variation near the ribs, etc.

A detailed investigation of the effect of ribs on the temperature field at the wall and, in particular, on the thermal streaks on the surface, is crucial for understanding the mechanism of heat removal from the ribbed wall to a fluid. Such data are, however, very scarce.

The aim of the present study is to fill this gap. Using infrared thermography, we obtained detailed information on the evolution of the temperature field at the wall near a single rib. We focused on the effect of the principal parameters on the structure of the thermal streaks, its distortion and restoration.

2. EXPERIMENTAL SET-UP

The experimental set-up and measurement technique were described earlier by Hetsroni and Rozenblit [15]. Therefore, we present here only the main parameters. The flow loop consisted of a stainless steel open flume, 4.3 m long, 0.32 m wide, and 0.1 m deep. Water at constant temperature ($20 \pm 0.1°C$) was recirculated within the flume (Fig. 1). The flow was provided by a centrifugal pump and was measured using an orifice plate. Care was taken to eliminate vibration,

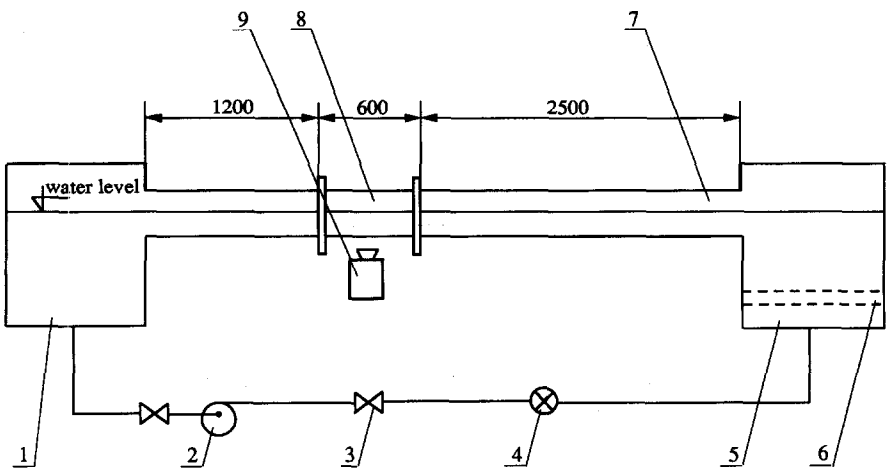

Fig. 1. Scheme of experimental set-up: 1, exit tank; 2, pump; 3, flow controlling valve; 4, flowmeter; 5, entrance tank; 6, grid; 7, flow development section; 8, test section; 9, infrared camera.

NOMENCLATURE

H	flow depth
h_x	local heat transfer coefficient behind a disturbance
h	heat transfer coefficient in the unperturbed flow
$\bar{h}$	non-dimensional heat transfer coefficient, $\bar{h} = h_x/h$
ℓ	width of the rib
N_x	number of thermal streaks in the spanwise direction in flow with a rib
N	number of thermal streaks in unperturbed flow
$\bar{N}$	non-dimensional thermal streaks, $\bar{N} = N_x/N$
Re	the Reynolds number, $Re = uH/\nu$
u	mean flow velocity
u^*	friction velocity $= \sqrt{\tau/\rho}$
x, y	longitudinal and vertical Cartesian coordinates
$\bar{x}$	non-dimensional distance from the rib, $\bar{x} = x/\ell$
x_1, x_2	coordinates of the front and rear boundaries of the relaxation region.

Greek symbols

δ	the length of the relaxation region, $\delta = x_2 - x_1$
θ	the angle between the rib and the flume bottom
Λ	thermal streaks spacing
Λ^+	non-dimensional thermal streaks spacing, $\Lambda^+ = \Lambda u^*/\nu$
ν	kinematic viscosity of the fluid
ξ	longitudinal coordinate behind the rib, $\xi = x - x_1$
$\bar{\xi}$	non-dimensional coordinate, $\bar{\xi} = \xi/\delta$
ω	an irregularity coefficient.

wave formation at the inlet, and reflections from the outlet.

A fully developed flow (depth 0.05 m) was established in the region beyond 2.5 m downstream from the inlet to the flume. This was confirmed by measurements of both the velocity profile and distribution of the RMS value of streamwise velocity fluctuations.

The measurements were performed at the centreline of the flume, i.e. at $z = 0$ (z is the spanwise coordinate). Velocity measurements were made by means of a hot-film anemometer. The standard 90° conical probe was connected to a traversing mechanism having a spatial resolution of 10 μm. The anemometer signal was transmitted in digital form through an acquisitor to a PC.

The heated section (a part of the channel which was

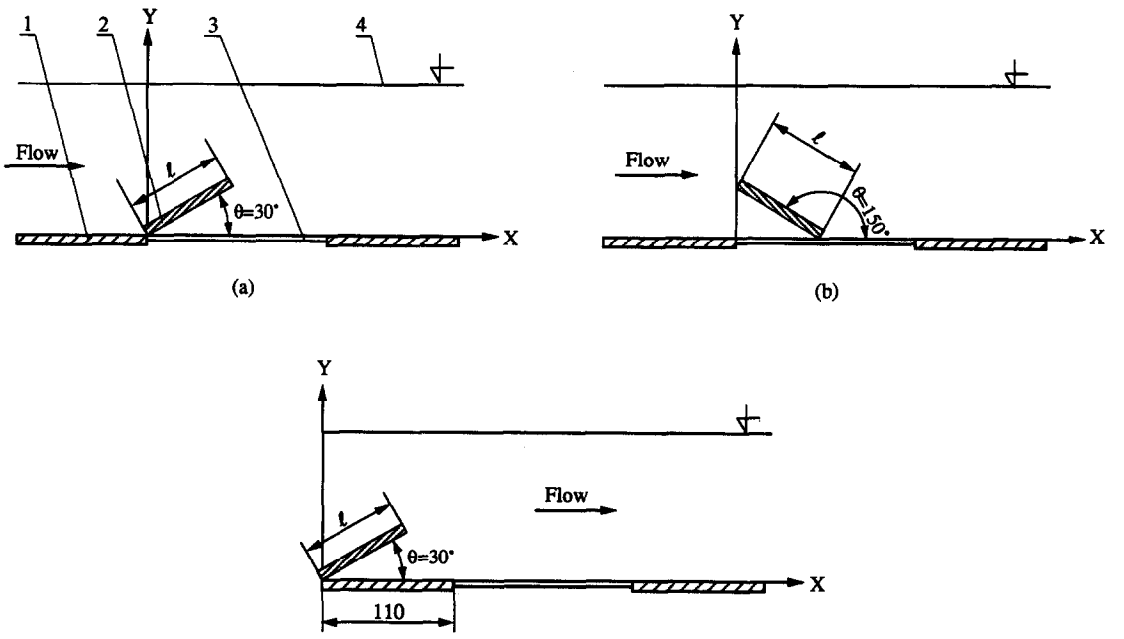

Fig. 2. Test section: 1, bottom of the flume; 2, rib; 3, electrical heater; 4, water surface. a,b,c, different orientations of the rib relative heater.

heated) was located at a distance of 2.5 m from the channel entrance. The constantan heater (on an isolated frame) was made of a foil 0.33 m long, 0.2 m wide, and 50 μm thick. The window of the frame was 0.3 m long and 0.15 m wide. The foil was attached to the window by means of a contact adhesive and was coated on the air side with black mat paint of about 20 μm thickness. Constancy of heat flux was achieved by supplying DC power.

The IR image of the heater was recorded from below. Since the heater was very thin (50 μm) and had almost no thermal inertia, it had a temperature virtually identical to that at the other side. Therefore, the temperature which we measured was almost the same as the temperature on the bottom of the flume at $y^+ = 0$ ($y^+ = yu^*/\nu$). There was a temperature difference between the two sides of the heater of about 0.1°C (Hetsroni and Rozenblit [15]).

The perturbations of the near-wall flow were introduced by means of cross ribs ($\ell = 10$ mm, $\ell = 20$ mm) 250 mm long, 2 mm thick, made of perspex. The ribs were fixed to the bottom of the flume at $y^+ = 0$.

Two locations for the ribs were selected. For both rib dimensions, the slope angles were taken to be 30° and 150° (Fig. 2).

The experiments with the rib of $\ell = 20$ mm were carried out at Reynolds number $Re = 3100$. In experiments with the rib of $\ell = 10$ mm, the Reynolds number was varied between 3100 and 8500.

Flow visualization, by means of the micro-bubble technique, was used. The bubbles were produced on a horizontal wire which was suspended in the test section and could be moved in the streamwise direction. Flow patterns were recorded by means of a video camera. The video was then used in play back mode to analyze the data.

We used a pulsed voltage across a 0.05 mm platinum wire (in a manner outlined by Kline *et al.* [16]) to produce hydrogen-bubble visualization streak-lines in the flow.

The thermal streak patterns and the instantaneous temperature variation on the heated foil were observed by means of an IR camera. Visual information was recorded using a video camera at a recording rate of 50 frames s^{-1}. The streaks were counted by using the identification criteria of Smith and Metzler [17].

The wall and flow temperatures were measured with an accuracy of ± 0.1°C. The error in the Reynolds number did not exceed $\pm 4\%$. The accuracy of determination the heat transfer coefficient was $\pm 12\%$. The accuracy of the estimation of the thermal streaks number, was $\pm 22\%$.

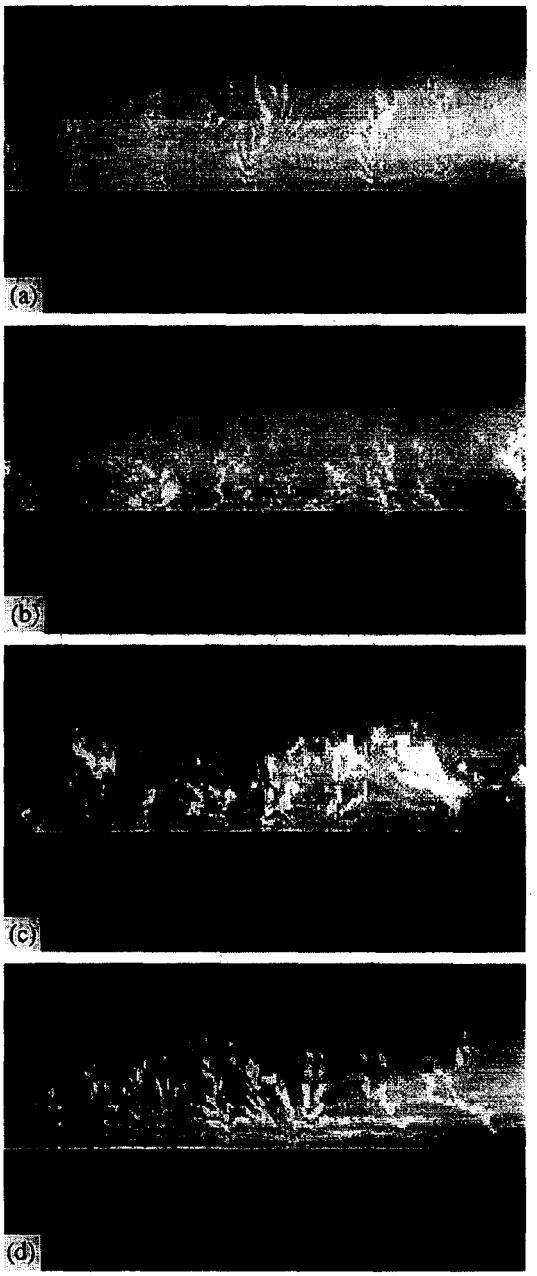

Fig. 3. Flow structure: a, in front of the rib $x/\ell = -7$; b, behind the rib $x/\ell = 4$; c, behind the rib $x/\ell = 10$; d, behind the rib $x/\ell = 16$.

3. RESULTS AND DISCUSSION

3.1. *Hydrodynamic structure of the flow*

The features of the near-wall flow structure upstream and downstream of the rib are illustrated in Fig 3(a)–(d). In these diagrams, the results of flow visualization using the microbubble technique are shown. The comparison of the data corresponding to flow upstream and downstream of the rib shows essentially different fluid motion in these regions. In Fig. 3(a) the regular flow structure (periodic in the spanwise direction) is observed. In Fig. 3(a) one can clearly see the domains of slow and rapid fluid motion, corresponding to low and high velocity streaks. Figure 3(b) corresponds to the region at a distance $\bar{x} = 4$ downstream of the rib. In the wake of the rib, the

streaky structure is disturbed and a quasi-homogeneous flow structure with random fluctuations of velocity is observed.

Far from the rib, the effect of the perturbations decreases. At large enough distances from the rib [downstream at $\bar{x} = 10$, Fig. 3(c)] the initial regular field near the rib may be represented (approximately) as a combination of an unperturbed motion, an irregular quasi-homogeneous flow (near the rib), and a relaxation zone in which restoration of the regular flow structure takes place. In the region at $\bar{x} \geqslant 16$ behind the rib, the flow pattern corresponds to conditions of unperturbed flow, Fig. 3(d).

3.2. *The thermal structure at the wall*

The features of the temperature distribution on the wall are depicted in Fig. 4(a) and (b), where the data on thermal streak distribution are presented. It is seen that in the unperturbed part of the flow, the number of thermal streaks is constant in the streamwise direction. In the region downstream of the rib the thermal streaks are totally disrupted, and in the relaxation region the number of thermal streaks increases again.

The distribution of the heat transfer coefficient is more complex. In Fig. 5 it is seen that the heat transfer coefficient changes non-monotonically in the region of irregular motion. The latter is probably due to the interaction of macro-scale vortices downstream of the rib and the wall. Notice that at a large distance from the rib the value of the heat transfer coefficient is higher than in the unperturbed flow in front of the rib. This suggests conservation of the structure of the macro-vortices behind the rib, and indicates its effect on the flow at large distance downstream.

Variation in the number of thermal streaks along the wall (near the rib) is illustrated in Fig. 6. These data show that the number of thermal streaks in front of the rib and far from it is practically identical. However, behind the rib (at the distance $0 < \Delta\bar{x} < 12$, $\Delta\bar{x} = \bar{x} - \bar{x}_1$) the thermal streaks are absent. At $12 < \Delta\bar{x} < 28$ (corresponding to the relaxation region) the number of thermal streaks increases to a value corresponding to the unperturbed flow $\bar{N} = 1$.

4. PHENOMENOLOGICAL DESCRIPTION

We now propose a simplified approach to estimating the number of thermal streaks downstream of a single rib situated in the near-wall region of a turbulent boundary layer. It is based on the assumption of a regular thermal structure on the wall surface. This approach also assumes that the temperature distribution on the wall has a streaky structure without an external perturbation.

To estimate the number of thermal streaks in the relaxation zone of the flow, we introduce the irregularity coefficient ω characterizing the deviation of N_x from its unperturbed value:

$$\omega = 1 - N_x/N \tag{1}$$

where N_x and N are the local number of thermal streaks and the number of thermal streaks in unperturbed flow.

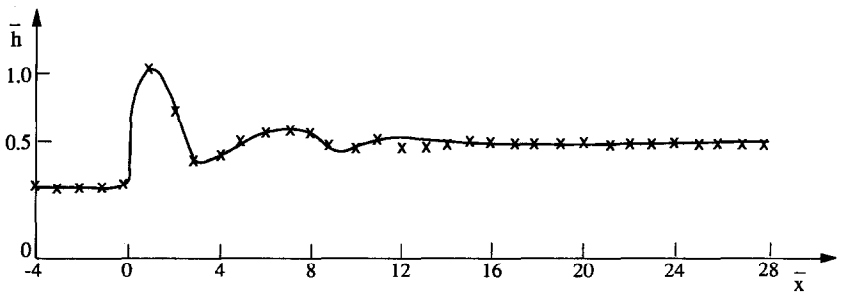

Fig. 5. Heat transfer coefficient distribution.

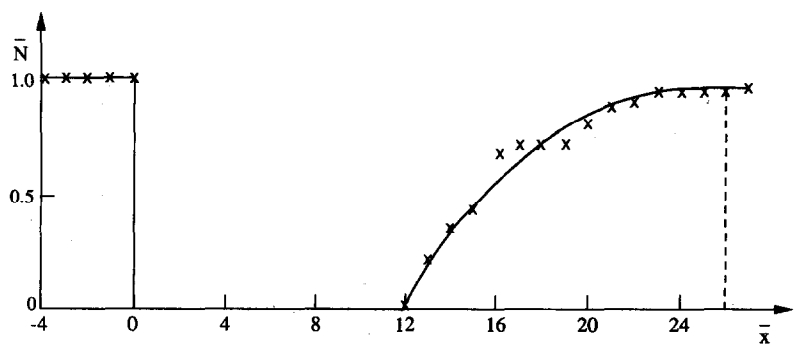

Fig. 6. The number of thermal streaks changing along wall (near the rib).

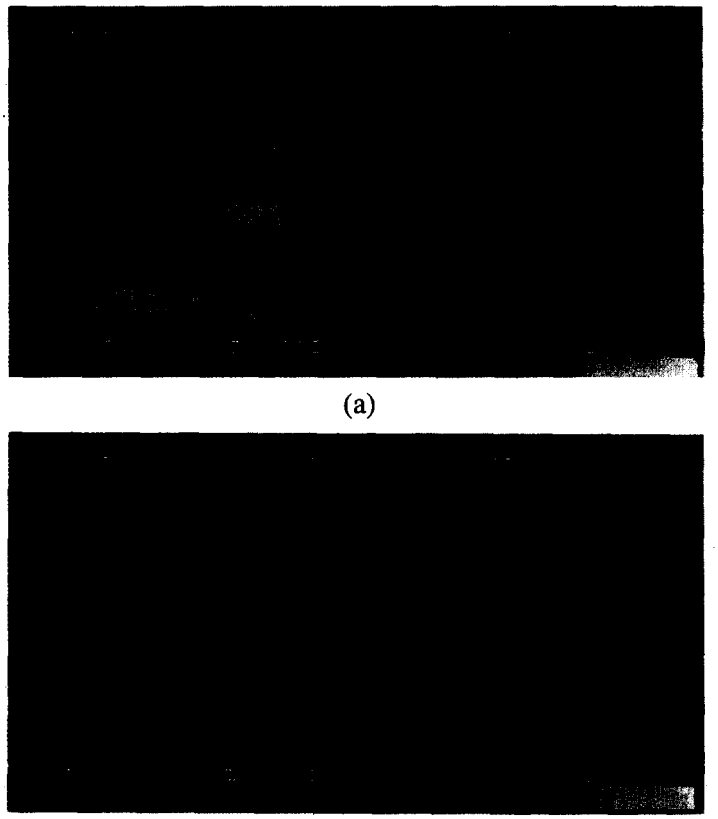

(a)

(b)

Fig. 4. Structure of the temperature field at the wall surface: a, in front of the rib $x/\ell = -7$ and behind the rib, $x/\ell \leqslant 10$; b, behind the rib $10 \leqslant x/\ell < 28$.

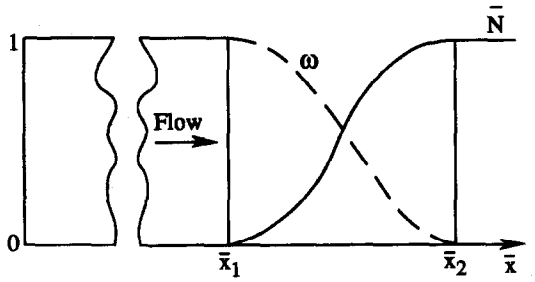

Fig. 7. Dependences $\bar{N}$, and ω on X.

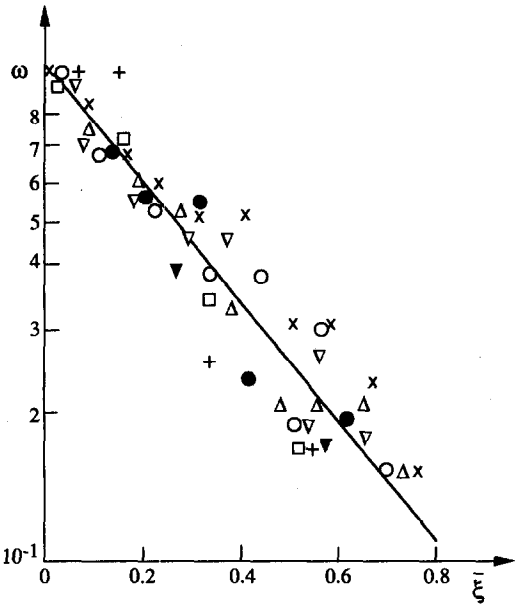

Fig. 8. Dependence ω on $\bar{\xi}$. (a) ●—$Re = 10 \times 10^3$; Δ—$Re = 8.4 \times 10^3$; X—$Re = 4.7 \times 10^3$; ○—$Re = 3.1 \times 10^3$. (b) □—$Re = 10 \times 10^3$; +—$Re = 8.4 \times 10^3$; ▼—$Re = 4.7 \times 10^3$. (c) ▽—$Re = 3.1 \times 10^3$. a,b,c corresponds to rib orientations shown in Fig. 2.

The dependence of ω ($\bar{x}$) on the distance downstream of disturbance (in the relaxation zone) is shown in Fig. 7(a). It is seen that ω monotonically decreases from its initial value $\omega = 1$ at the beginning of this region to the final value $\omega = 0$ at some distance from the disturbance.

For further analysis of the problem we present the dependence of $\omega = \varphi(\bar{\xi})$ in the $(d\omega/d\bar{\xi}, \omega)$ plane. In this case the equation determining ω is:

$$\frac{d\omega}{d\bar{\xi}} = f(\omega) \tag{2}$$

where $\bar{\xi} = (x - x_1)/\delta$, and $\delta = x_2 - x_1$ is the characteristic scale of the relaxation zone: x_1 and x_2 are the coordinates of the front and rear boundaries of the relaxation region, respectively.

Consider the behaviour of the function $\omega(\bar{\xi})$ in the neighborhood of the steady state, i.e. at $\bar{\xi} = 1$, $\omega \approx 0$. Expanding it in a Taylor series $f(\omega) = f(0) + (\omega/1!)f'(0) + (\omega^2/2!)f'(0)$ (omitting the terms of higher order), we arrive at the following equation (with $f(0) \equiv 0$; $f'(0) < 0$)

$$\frac{d\omega}{d\bar{\xi}} = -\alpha^2 \omega \tag{3}$$

where $\alpha^2 = |f'(0)|$.

Integration of equation (3) yields

$$\omega = \exp(-\alpha^2 \bar{\xi}). \tag{4}$$

Equation (4) shows that the logarithm of ω is linearly proportional to the non-dimensional variable $\bar{\xi}$. The

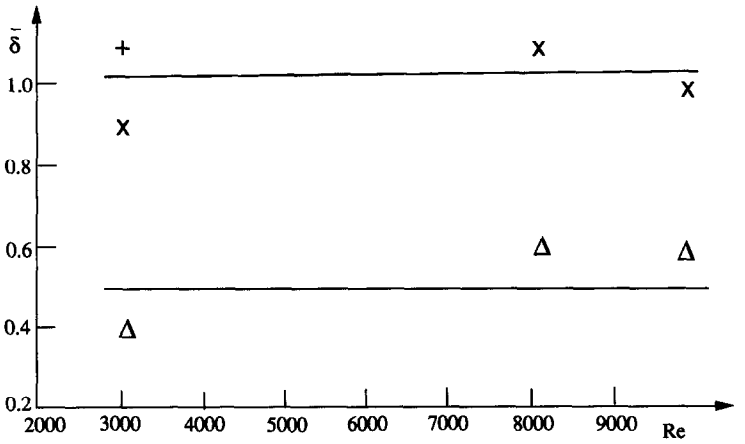

Fig. 9. Dependence of length of the relaxation region on Re. (a) x—$\ell = 10^{-2}$ m; (b) △—$\ell = 10^{-2}$ m; (c) +—$\ell = 2.10^{-2}$ m. a,b,c corresponds to rib orientations shown in Fig. 2.

experimental data on the dependence ω on $\bar{\xi}$ are plotted in Fig. 8. It is seen that all the data points for the various flow conditions are grouped near the line corresponding to equation (4). The characteristic scale of the relaxation regions, $\bar{\delta} = \delta/\ell$, does not depend on the Reynolds number and is determined by the rib orientation only, see Fig. 9.

5. CONCLUSIONS

An experimental study was carried out to explore the temperature field on a wall, near a single rib, in a developed turbulent flow. The following results were obtained:

(1) The rib on the wall surface effects the heat transfer in the turbulent boundary layer. The effect of the rib manifests itself in the changing of hydrodynamic and thermal fields, disturbing the thermal streaks near the rib, and a sharp increase of the heat transfer coefficient in this region.

(2) Behind the rib (at $\Delta\bar{x} \sim 10$) there is a relaxation region in which the thermal streaks are restored. The complete thermal structure is observed at $\Delta\bar{x} \sim 25$.

(3) The number of thermal streaks in the relaxation region changes as $\omega = \exp(-\alpha^2\bar{\xi})$.

Acknowledgements—This research was supported by a grant from the Ministry of Science and the Arts; by the Technion VPR Fund, Israel–Mexico Energy Research Fund; and by the Fund for the Promotion of Research at the Technion. A. Mosyak is partially supported by the Center for Absorption in Science, Ministry of Immigrants Absorption, State of Israel. L. P. Yarin is supported by the Israel Council for Higher Education.

REFERENCES

1. Kakac, S., Shah, R. K. and Aung, W., *Handbook of Single Phase Convective Heat Transfer*. Chap. 17. Wiley, New York, 1987.
2. Zukauskas, A., *High-Performance Single-Phase Heat Exchangers*. Hemisphere, New York, 1989.
3. Webb, R. L., *Principles of Enhanced Heat Transfer*. Wiley, New York, 1994.
4. Sparrow, E. M. and Tao, W. Q., Enhanced heat transfer in a flat rectangular duct with streamwise-periodic disturbances at one principal wall. *ASME Journal of Heat Transfer*, 1983, **105**, 851–861.
5. Sparrow, E. M. and Tao, W. Q., Symmetric versus asymmetric periodic disturbances at the walls of a heated flow passage. *International Journal of Heat and Mass Transfer*, 1984, **27**, 2133–2144.
6. Han, J. C., Heat transfer and friction in channels with two opposite rib-roughness walls. *ASME Journal of Heat Transfer*, 1984, **106**, 774–781.
7. Han, J. C., Heat transfer and friction characteristics in rectangular channel with rib turbulators. *ASME Journal of Heat Transfer*, 1988, **110**, 321–328.
8. Han, J. C., Ou, S., Park, J. S. and Lei, C. K., Heat transfer enhancement in channels with turbulent promoters. *ASME Journal of Engineering for Gas Turbines and Power*, 1985, **107**, 628–635.
9. Metzger, D. E., Fan, C. S. and Yu, Y., Effects of rib angle and orientation on local heat transfer in square channels with angled roughness ribs. In: *Compact Heat Exchangers*. A Festschrift for A. L. London, Hemisphere Publishing Corporation, New York, 1990, pp. 151–167.
10. Hishida, M. and Takase, K., Heat transfer coefficient of the ribbed surface. In *Proceedings of the ASME/JSME. Thermal Engineering Conference*, Vol. 3, 1991 pp. 100–103.
11. Liou, T. M. and Hwang, J. I., Turbulent heat transfer augmentation and friction in periodic fully developed channel flows. *ASME Journal of Heat Transfer*, 1992, **114**, 56–64.
12. Hirota, M., Fujita, H. and Yokosawa, Y., Experimental study on convective heat transfer for turbulent flow in a square duct with a ribbed rough wall (characteristics of mean temperature field). *ASME Journal of Heat Transfer*, 1994, **116**, 332–340.
13. Aliaga, D. A., Lamb, J. P. and Klein, D. E., Convection heat transfer distributions over plates with square ribs from infrared thermography measurements. *International Journal of Heat and Mass Transfer*, 1994, **37**, 363–374.
14. Lorenz, S., Mukomilow, D. and Leiner, W., Distribution of the heat transfer coefficient in a channel with periodic transverse grooves. *Experimental Thermal and Fluid Science*, 1995, **11**, 234–242.
15. Hetsroni, G. and Rozenblit, R., Heat transfer to liquid–solid mixture in a flume. *International Journal of Multiphase Flow*, 1994, **20**, 671–689.
16. Kline, S. J., Reynolds, W. C., Schraub, F. A. and Runstadler, P. W., The structure of turbulent boundary layers. *Journal of Fluid Mechanics*, 1967, **30**, 741–773.
17. Smith, C. R. and Metzler, S. P., The characteristics of low-speed streaks in the near-wall region of a turbulent boundary layer. *Journal of Fluid Mechanics*, 1983, **129**, 27–54.